


Solvent-regulable interfacial groups enable on-demand superhydrophobic/superhydrophilic silica aerogels

Received: 27 August 2024

Accepted: 13 February 2025

Published online: 05 March 2025

 Check for updatesLixiao Chen^{1,2,4}, Lishan Li^{2,4} & Xuotong Zhang^{2,3} 

Silica aerogel, as the earliest synthetic and commercially available one among all known aerogels, holds significant value in fields including thermal and acoustic insulation, optics, catalysis, sorption, etc. However, throughout its nearly century-long history, the influence of solvent used during synthesis on the properties of silica aerogels has been neglected, resulting in inaccurate and ambiguous performance evaluation. Herein, we have uncovered and systematically investigated the solvent-regulable interfacial groups that enable on-demand superhydrophobicity/superhydrophilicity of silica aerogels. During either sol-gel transition or solvent exchange process both required for aerogel synthesis, the alteration of solvent either from water to ethanol or vice versa leads to silica interfacial groups switch from superhydrophilic Si-OH to superhydrophobic Si-OEt or reversely due to reversible esterification, thus enabling on-demand superhydrophobic/superhydrophilic silica aerogels. It is worth noting that on-demand solvent-regulated hydrophilicity/hydrophobicity holds true regardless of used silica precursors (the mixture of trimethoxymethylsilane (MTMS)/tetramethoxysilane (TMOS), MTMS/tetraethyl orthosilicate (TEOS), or sodium methicosilicate (SMS)/TMOS), thereby indicating its universality, which wakes up considerable attention for producers involved in silica aerogels. Additionally, the discovery also provides a green, economical, and efficient way to achieve silica aerogels with on-demand hydrophilic/hydrophobic performance for specific sorption, etc.

Aerogels are a vital kind of mesoporous nanomaterials, one of the ten emerging materials that will change the world, listed in *Science*¹. Since first appearance of silica aerogels in 1931, a wide range of aerogels have been explored and extensively applied²⁻⁷. Among these different varieties, silica aerogels, being the earliest developed and extensively investigated, have undergone systematic exploration and rapid commercialization⁸. In academic aspect, silica aerogels possess distinctive characteristics such as high porosity, large specific surface area, low thermal conductivity, adjustable reflectivity, and scattering rate, as well as a low sound velocity due to their controllability in terms of

building block size, pore structure, and three-dimensional (3D) branched network. In the commercial aspect, the unique properties of silica aerogels enable their wide application in environmental restoration⁹, thermal insulation¹⁰, optics¹¹, and acoustics¹². Silica aerogel products, such as monolith¹³, granule¹⁴, powder¹⁵, blanket¹⁶, and coating¹⁷, are extensively utilized in the aerospace industry^{18,19} as well as in manufacturing sectors²⁰ and buildings^{21,22}. These diverse applications establish the crucial role of silica aerogels in high-tech fields and economic development.

Conventional synthetic routes on silica aerogels are based on the sol-gel transition of their precursors and gel aging in mother liquor,

¹School of Nano-Tech and Nano-Bionics, University of Science and Technology of China, Hefei, PR China. ²Suzhou Institute of Nano-tech and Nano-bionics, Chinese Academy of Sciences, Suzhou, PR China. ³College of Textile Science and Engineering, Jiangnan University, Wuxi, PR China. ⁴These authors contributed equally: Lixiao Chen, Lishan Li. ✉ e-mail: xtzhang2013@sinano.ac.cn

followed by solvent exchange and supercritical (Sc) drying or ambient pressure drying in sequence. The general sol-gel transition of silica precursors can be classified into one-step and two-step strategies. The one-step strategy involves direct hydrolysis and condensation in an acidic or basic solution, while the two-step strategy entails hydrolysis of silica precursors in an acidic solution followed by sequential condensation in an alkaline solution⁸. Up to now, most efforts are concentrated on exploring suitable reactants (such as silica precursors²³, catalyst²⁴, et al.) during the sol-gel process to tune the aerogel structures including building block sizes, pore geometry, and 3D networks to satisfy requirements for specific application scenarios²⁵. Solvent, serving as reaction and drying media, plays crucial roles in the preparation of silica aerogels²⁶. Various solvent treatments in sol-gel transition, solvent exchange, and Sc drying are required during the preparation of silica aerogels. For instance, a sequential treatment involving water and alcohol is commonly employed to effectively eliminate impurities such as inorganic salts²⁷. It is generally believed that under mild solvent (water, ethanol) conditions, the chemical and physical properties of silica aerogels are stable. Only under harsh conditions (high temperature, high pressure, strong catalyst, etc.), the properties of silica aerogels will change greatly. For example, researchers have discovered that under harsh Sc conditions (240–245 °C), or strong acid-base catalysis, the silicon hydroxyl groups can be esterified with alcohols^{28–31}, so as to achieve hydrophobic silica aerogels. However, despite its nearly century-long history, Nobody has reported that water/alcohol in the mild solvent process could lead to dramatic changes in the properties of silica aerogels, leading to inaccurate and ambiguous performance assessments of them.

In this work, we comprehensively and systematically studied the solvent-regulated hydrophilic-hydrophobic interfacial group transitions during reaction and solvent exchange processes, and consequent fabrication of on-demand superhydrophobic (with water contact angle $\geq 150^\circ$ as well as water sliding angle $\leq 10^\circ$)/superhydrophilic silica aerogels using a mixture of MTMS and TMOS as silica precursors (Fig. 1). During synthesis, hot water, and ethanol were employed as the reaction or exchange solvents to investigate the impact of mild solvents on the surface attribute of aerogel. The hydrophilicity/hydrophobicity of aerogel depends on the choice of hot water/ethanol used for the solvent treatment of the wet gel before Sc CO₂ drying. The utilization of hot water results in the formation of wet hydrogel and subsequent superhydrophilic aerogel (SL-A) after Sc CO₂ drying, while employing hot ethanol leads to the production of wet organogel and

subsequent superhydrophobic aerogel (SB-A) after Sc CO₂ drying. To distinguish them from regular wet gels, we here define wet hydrogel as SL-A precursors, and organogels as SB-A precursors. Therefore, the repetitive hot water/ethanol switching during the solvent exchange of the wet gel facilitates multiple switchable transitions between SL-A and SB-A precursors, thereby enabling on-demand SL and SB-As. The mechanism study indicates that such switchable SL-A and SB-A precursors are due to reversible esterification between Si-OH and ethanol. It is worth noting that this significant finding holds true for a wide range of silica precursors (the mixture of MTMS/TMOS, MTMS/TEOS, and SMS/TMOS), thereby indicating its universality in the preparation of silica aerogels. Additionally, the discovery also provides a green, economical, and efficient way to achieve on-demand SL/SB-As.

Results

Switchable SL-A/SB-A precursor transitions and on-demand aerogel superhydrophobicity/superhydrophilicity

The fabrication of silica aerogels includes three steps: sol-gel transition of silica precursors and aging, solvent exchange, and Sc CO₂ dry. The three-dimensional porous skeleton formed via the sol-gel process can be preserved during the Sc drying process, thereby ensuring the successful formation of aerogels. For instance, here, the sol-gel transition and aging were performed with MTMS and TMOS as silica co-precursors, via hydrolyzation in hydrochloric acid at room temperature and condensation in ammonia aqueous and aging in mother liquor at 80 °C for 48 h. During solvent exchange, water, and ethanol were chosen as common solvents respectively depending on specific occasions, and sometimes, heating is necessary to accelerate the mass transfer rate. Two routes were designed using ethanol (Fig. 2a) and water (Fig. 3a) as reaction solvents to study the solvent effect during sol-gel transition and aging process. Likewise, hot ethanol and hot water were repeatedly switched in the solvent exchange progress to study the effect of solvent in this progress.

In synthetic route 1, alcohol was commonly used in the sol-gel process for organosiloxane precursors (Fig. 2a). The structures and surface attributes of aerogel fabricated with ethanol as a sol-gel solvent were first studied in detail. As illustrated in Fig. 2a, under acid-base catalysis, the co-precursors of MTMS and TMOS undergo hydrolysis and condensation in sequence to form SB-A precursors. Following Sc CO₂ drying, translucent superhydrophobic silica aerogels were obtained with density of $0.127 \pm 0.004 \text{ g/cm}^3$ (Fig. 2b). Such aerogel networks were composed of silica primary particles with a radius of

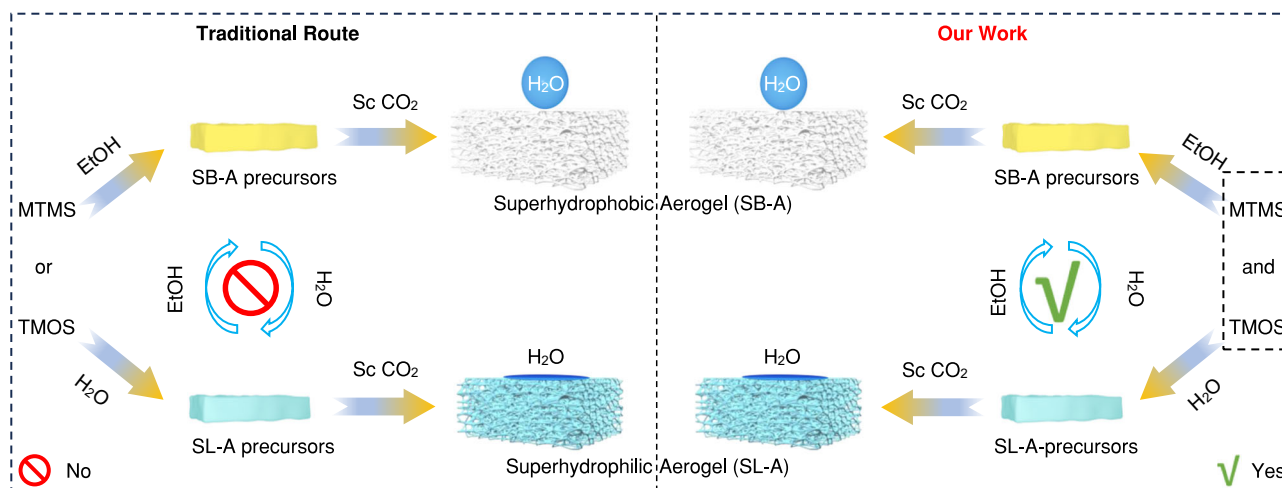


Fig. 1 | Comparison between the traditional route and our route. Schematic illustration of solvent-regulated switchable superhydrophobic–hydrophilic silica aerogels precursor transitions and synthesis of on-demand superhydrophobic/superhydrophilic aerogels reported in our study vs. synthesis of traditional silica

aerogels without SB-A/SL-A precursor transitions. MTMS trimethoxymethylsilane, TMOS tetramethoxysilane, EtOH ethanol, SB-A superhydrophobic aerogel, SL-A superhydrophilic aerogel, Sc CO₂ supercritical CO₂.

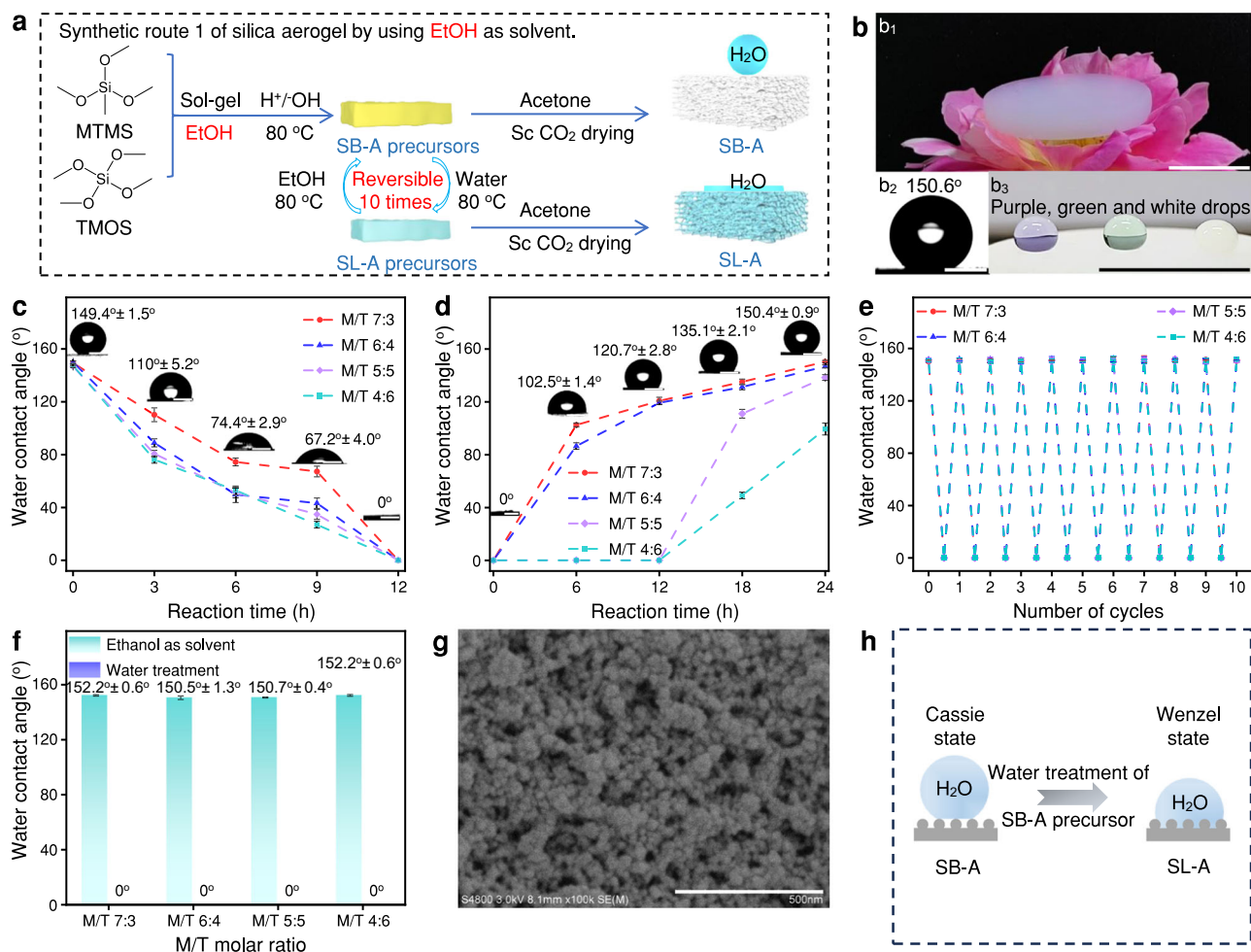


Fig. 2 | Switchable SL-A/SB-A precursor transitions and corresponding superhydrophobic/superhydrophilic silica aerogels. SB-A superhydrophobic aerogel, SL-A superhydrophilic aerogel. **a** Synthesis route of on-demand superhydrophilic/superhydrophobic silica aerogels with switchable SL-A/SB-A precursor transition by using ethanol as reaction solvent. MTMS trimethoxymethylsilane; TMOS tetramethoxysilane, EtOH ethanol, Sc CO₂ supercritical CO₂. **b** Photographs of silica aerogels (**b**₁) and water contact angle on superhydrophobic silica aerogels (**b**₂) and droplets with diverse color standing on silica aerogels (**b**₃). Scale bar: **b**₁ and **b**₃: 1 cm; **b**₂: 500 μm. **c** Water contact angles of silica aerogels from SB-A precursor after hot water treatment for different times. Scale bar: 500 μm. Error bar: <6.0°. **d** Water

contact angles of silica aerogels from SL-A precursor after hot ethanol treatment for different times. Scale bar: 500 μm. Error bar: <4.5°. **e** Water contact angles of silica aerogels from cyclic SL-A/SB-A precursor transitions by treating wet gels alternately with hot water/ethanol. Error bar: <2.6°. **f** Water contact angles of silica aerogels with diverse M/T molar ratios from initial SB-A precursors (left) and water-induced SL-A precursors (right). M/T: MTMS: TMOS. **g** SEM image of silica aerogel from initial SB-A precursor. Scale bar: 500 nm. **h** Illustration of Cassie state to Wenzel state transition of silica aerogel from the initial SB-A precursor to the water induced SL-A precursor. Source data are provided as a Source Data file.

about 3.30 ± 0.61 nm with large specific surface area and small pore widths (Supplementary Fig. 1). For example, the specific surface area is 1047 m²/g for samples obtained by co-precursors with a molar ratio of MTMS/TMOS (M/T) 7:3, 1036 m²/g for that of M/T 6:4, 759 m²/g for that of M/T 5:5 and 803 m²/g for that of M/T 4:6, respectively. Also, the adsorption average pore widths of such silica aerogels are 7.3 nm for that of M/T 7:3, 9.3 nm for that of M/T 6:4, 10.6 nm for that of M/T 5:5 and 11.3 nm for that of M/T 4:6, respectively, similar to or higher than reported data³². Superhydrophobicity of aerogel was reflected directly by water contact angle as high as $150.6^\circ \pm 0.2^\circ$ (Fig. 2b₂), with water sliding angle as low as $2.9^\circ \pm 0.8^\circ$ and multiple water droplet resilience (Supplementary Figs. 2 and 3). Hence, water droplets dyed with purple, green or white pigments can never infiltrate into such superhydrophobic silica aerogels (Fig. 2b₃ and Supplementary Fig. 4). However, during the solvent exchange process, if ethanol in the SB-A precursor was completely substituted with water and holding it at 80 °C for a specific duration, followed by Sc CO₂ drying, gradual formation of superhydrophilic silica aerogel can be achieved. The water contact angles of obtained silica aerogels are negatively correlated with the hot

water treatment time for SB-A precursors. As illustrated in Fig. 2c, with an increase of water treatment time for SB-A precursor, water contact angles of the obtained silica aerogels decrease gradually, reducing from 149.4° to 110.1° , 74.4° , 67.2° and even 0° for samples prepared with the molar ratio of M/T 7:3 after 72 h, which displays great potential in on-demand surface attribute regulation from SB-A to SL-A precursors. Additionally, the SB-A precursors and corresponding superhydrophobic silica aerogels can be reobtained by resubstituting water in SL-A precursor with ethanol, holding it at 80 °C for a specific duration, and Sc CO₂ drying. During the transition from SL-A to SB-A precursors, Water contact angle of relative aerogel increases gradually from 0° , 102.5° , 120.7° , 135.1° to 150.4° (Fig. 2d). Such water-induced SL-A precursors and the ethanol-induced recuperative SB-A precursors are switchable and can be fully cycled for at least ten loops (Fig. 2e). These SB-As exhibit consistent static water contact angles of $150.8^\circ \pm 0.9^\circ$ and water sliding angles of $5.8^\circ \pm 1.4^\circ$, and SL-A have constant water contact angles of 0° , indicating the stability and reversibility of these cyclic processes (Supplementary Fig. 5a). Beyond the molar ratio of M/T of 7:3, such water-induced transition from SB-A

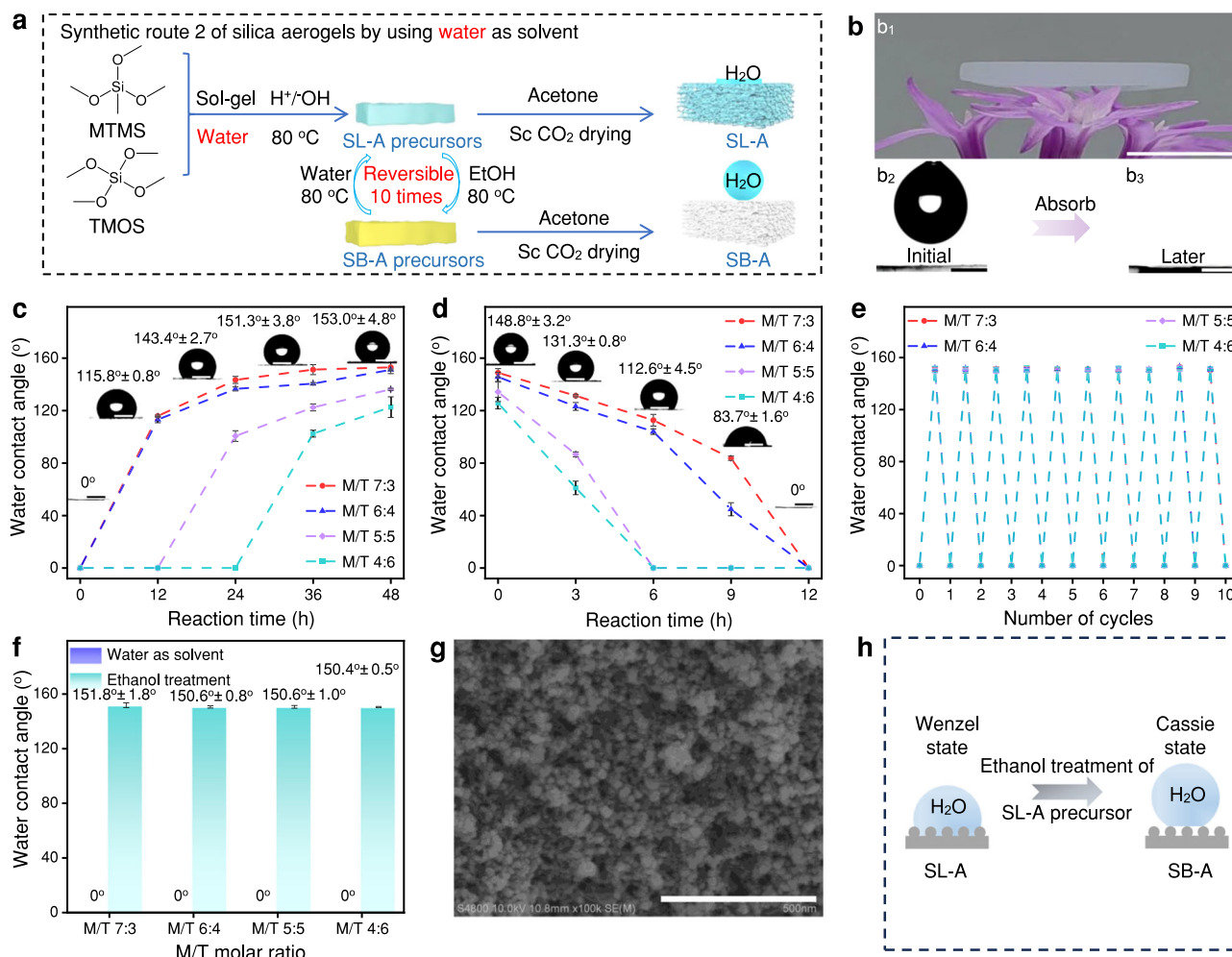


Fig. 3 | Switchable SL-A/SB-A precursor transitions and corresponding superhydrophobic/superhydrophilic silica aerogels. SB-A superhydrophobic aerogel, SL-A superhydrophilic aerogel. **a** Synthetic route of on-demand superhydrophilic/superhydrophobic silica aerogels with switchable SL-A/SB-A precursor transition by using water as a reaction solvent. MTMS trimethoxymethylsilane, TMOS tetramethoxysilane, EtOH ethanol, Sc CO_2 supercritical CO_2 . **b** Photographs of silica aerogels (**b**₁) and water contact angles on superhydrophilic silica aerogels initially (**b**₂) and later (**b**₃). Scale bar: **b**₁: 1 cm; **b**₂ and **b**₃: 500 μ m. **c** Water contact angles of silica aerogels from SL-A precursor after hot ethanol treatment for different times. Scale bar: 500 μ m. Error bar: <7.9°. **d** Water contact angles of silica aerogels from

SB-A precursor after hot water treatment for different times. Scale bar: 500 μ m. Error bar: <7.4°. **e** Water contact angles of silica aerogels from cyclic SL-A/SB-A precursor transitions by treating wet gels alternately with hot ethanol/water. Error bar: <2.5°. **f** Water contact angles of silica aerogels with diverse M/T molar ratios from initial SL-A precursors (left) and ethanol-induced SB-A precursors (right). M/T: MTMS: TMOS. **g** SEM image of silica aerogels from initial SB-A precursor. Scale bar: 500 nm. **h** Illustration of Wenzel state to Cassie state transition of silica aerogel from initial SL-A precursor to ethanol-induced SL-A precursor. Source data are provided as a Source Data file.

to SL-A precursors and formation of SL-A were applicable to other ratios of M/T of 5:5, 6:4, and 4:6, indicating the universality of the phenomenon (Fig. 2f and Supplementary Fig. 5b).

The inner network structures of superhydrophobic silica aerogel from initial SB-A precursor and SL-A from the water-induced SL-A precursor were tracked for better understanding the wetting behavior of these aerogels. From the scanning electron microscopy (SEM) images and 3D confocal microscope images, it is evident that all aerogel surfaces exhibit rough morphologies (Fig. 2g and Supplementary Figs. 6–8). To gain deeper insights into the wetting behavior transition from superhydrophobic to SL-A, the Cassie-Wenzel wetting model was employed. For SB-A with a water contact angle of 150° and a water sliding angle of 3.66°, water droplets did not infiltrate into the aerogel pores but instead rolled off rapidly down an incline, akin to the lotus leaf effect. This behavior can be effectively explained by the Cassie model. As the water treatment time increased, the water contact angle decreased slightly to 149° while the water sliding angle gradually increased to 15.38°. With further prolonged water treatment, the water contact angle continued to decrease to 127°, and droplets no longer

rolled off even when the aerogel was inverted 180°, indicating a high adhesion state similar to the petal effect. According to literature, possible wetting states at this stage include the Wenzel state with strong pinning sites^{33–35}. Upon extended water treatment, SL-A with a water contact angle of 0° was obtained, where water droplets fully infiltrated the aerogel pores (Supplementary Fig. 9). Consequently, its wetting behavior can be well described by the Cassie-Wenzel model. The results demonstrate that as water treatment time increases, the wetting state of water droplets on the aerogel surface transitions from the Cassie state to the Wenzel state (Fig. 2h).

Water was another common solvent used in sol-gel process for silica precursors in synthetic route 2 (Fig. 3a). To further validate feasibility of solvent-regulable SL-A/SB-A precursor transitions and on-demand superhydrophobicity/superhydrophilicity controlling, we synthesized silica aerogels directly using water as solvent at sol-gel transition step. As illustrated in Fig. 3a, in water, the above-mentioned same precursor mixture of MTMS and TMOS first hydrolyze in dilute hydrochloric acid and then condense in ammonium hydroxide to form SL-A precursor. Followed with Sc CO_2 drying, superhydrophilic silica

aerogels with density among ($0.113 \pm 0.004 \text{ g/cm}^3$) are obtained. It is worth noting that at same conditions with route 1 in Fig. 2a, here, only changing the solvent in the sol-gel transition process from ethanol to water led to the formation of superhydrophilic silica aerogels. Such silica aerogels are translucent (Fig. 3b) and water droplet will be immediately adsorbed once contact with each other (Fig. 3b₂, b₃). Such aerogel networks were composed of silica primary particles with a radius of about 4.11 nm with specific surface area of 472 m²/g for silica aerogels prepared by co-precursors with molar ratio of M/T 7:3, 579 m²/g for that of M/T 6:4, 547 m²/g for that of M/T 5:5 and 567 m²/g for that of M/T 4:6, respectively. Also, their corresponding adsorption average pore width is 8.6 nm, 9.2 nm, 12.3 nm, and 8.5 nm respectively (Supplementary Fig. 10). Similar to the above phenomenon, if the water in SL-A precursors was substituted with ethanol under heating, SB-A precursors come into being and superhydrophobic silica aerogels are produced after Sc CO₂ drying. Under different treatment time in such process, water contact angles of the resulting silica aerogels change from 0° to 115.8°, 143.4°, 1501.2°, and 153.0° for M/T 7/3 silica aerogels (Fig. 3c). Also, superhydrophilic silica aerogel can be reobtained once ethanol in SB-A precursor was replaced with water during solvent exchange process, with water contact angles reducing from 148.8°, 131.3°, 112.6°, 83.7° and 0° for M/T 7/3 silica aerogels (Fig. 3d). Such ethanol-induced SB-A precursors and the water-induced recuperative SL-A precursors are switchable and can be fully cycled for at least ten loops (Fig. 3e) with water contact angle and sliding angle remain $151^\circ \pm 1^\circ$ and $6.5^\circ \pm 1.9^\circ$, respectively (Supplementary Fig. 11a) and multiple water droplet resilience (Supplementary Figs. 2 and 3). Same trends also happen to silica aerogels obtained by other molar ratios of M/T 6:4, 5:5, and 4:6, respectively, indicating the universality of the phenomenon again (Fig. 3f and Supplementary Fig. 11b).

Similarly, the inner network structures of superhydrophilic silica aerogel from the initial SL-A precursor and SB-A from ethanol-induced SB-A precursor were tracked for a better understanding the wetting behaviors of these aerogels. From the SEM and 3D confocal microscope images, all aerogel surfaces exhibit rough morphologies (Fig. 3g and Supplementary Figs. 12–14). The wetting behaviors from superhydrophilic to SB-As were also investigated. For SL-A with a water contact angle of 0°, water droplets infiltrate into the aerogel pores. As the ethanol treatment time increased, the water contact angle gradually rose to 113°, and the droplets exhibited high adhesion, which can be accurately described by the Wenzel model. With further increases in ethanol treatment time, the water contact angle increased to 150°, and water droplets began to roll on an inclined surface of aerogel at a water sliding angle of 15.38°. Finally, the water contact angle reached 151° with a reduced water sliding angle of 3.57°, indicating a transition to the Cassie state (Supplementary Fig. 15). These results demonstrate that the wetting behavior evolves from the Wenzel to the Cassie state as the ethanol treatment time extends.

Above all, solvent-regulable surface attribute change of silica aerogels was investigated by selecting different sol-gel routes and solvent exchange treatment. When using ethanol as sol-gel solvent, superhydrophobic silica aerogels were obtained. While, using water as sol-gel solvent, superhydrophilic silica aerogels were produced. Additionally, reversible transitions between SB-A precursor and SL-A precursor can be achieved by solvent exchange in ethanol and water respectively at 80 °C, resulting in on-demand superhydrophobic/superhydrophilic silica aerogels and tunable wetting behavior. In short, water induces the superhydrophilicity, and ethanol results in superhydrophobicity. All these confirm the feasibility of solvent-regulated switchable SB-A/SL-A precursor transitions and on-demand superhydrophobicity/superhydrophilicity of silica aerogels.

Reversible SL-A/SB-A precursor transition mechanism

It is well established that the wettability of a substrate surface is primarily influenced by two factors: surface chemical composition and

surface microstructure³⁶. SEM and 3D confocal images revealed no significant differences in the micro- and nano-scale surface morphologies between superhydrophilic and superhydrophobic silica aerogels, both exhibiting similar roughness values and spherical secondary particles (Supplementary Figs. 6–7 and 12–14). Therefore, it is reasonable to infer that the superhydrophobic and superhydrophilic properties of silica aerogels are predominantly attributed to variations in their surface chemical composition. To further explore the mechanisms, we use attenuated total reflection infrared (ATR-IR) spectra and solid-state nuclear magnetic resonance (NMR) spectra to characterize the chemical structure changes of such silica aerogels (Fig. 4). Based on these data analyses, we deduce that esterification reaction and its inverse reaction play a crucial role in the switchable SB-A precursor and SL-A precursor transition (Fig. 4a). Firstly, in the normalized ATR-IR spectra by standardized signals of absorbance at 1275 cm⁻¹ (vibration of Si-C groups)³⁷, the intensity of absorbance at 1035 cm⁻¹ (ascribing to stretching vibrations of Si-O and C-O groups) and absorbance at 2940 cm⁻¹ (ascribing to symmetric stretching vibrations of C-H from -OCH₂CH₃ groups) and absorbance at 2980 cm⁻¹ (ascribing to antisymmetric stretching vibrations of C-H from Si-CH₃ or Si-OCH₂CH₃ groups)^{38,39}, are comparatively weaker in superhydrophilic silica aerogels compared to their superhydrophobic counterparts (Fig. 4b). Simultaneously, the absorption bands at 3448 cm⁻¹ and 1638 cm⁻¹, associated with vibrations of O-H groups, exhibit stronger intensity in superhydrophilic silica aerogels than those superhydrophobic counterparts⁴⁰. The results indicate an abundance of C-O and C-H bonds on hydrophobic silica aerogels and -OH groups on hydrophilic silica aerogels, aligning well with the aforementioned hydrophobic/hydrophilic properties. Based on this, one rational hypothesis was proposed that in ethanol, the formation of -OCH₂CH₃ bonds are induced by condensation reactions between -OH groups and ethanol. Conversely, in water, hydrolysis of Si-O-C chemical bonds leads to the regeneration of -OH.

To exactly characterize chemical structure of superhydrophilic and superhydrophobic silica aerogels, NMR spectrum was tested. From ²⁹Si cross-polarization magic angle spinning NMR spectrum in Fig. 4c, for superhydrophobic silica aerogels and superhydrophilic ones, the signals of Q₄ (-112 ppm), Q₃ (-100 ppm) and T₃ (-65 ppm) and T₂ (-58 ppm) display no distinct difference, where Q_n denotes a tetrahedral Si with n bridging oxygens, T_n stands for a tetrahedral Si with 1C and n bridging oxygens⁴¹. This means that the switchable transition between superhydrophobic-superhydrophilic silica aerogel precursors does not change the Q_n or T_n species, that is, the bridging Si-O-Si bands are stable during hydrolysis/alcoholysis and the esterification and hydrolysis reactions mainly occur on Si-OH and Si-O-CH₂CH₃ groups. Furthermore, the strong signals at chemical shifts of 12 ppm and 53 ppm in the ¹³C NMR spectra indicated the existence of -OCH₂CH₃ groups⁴² in superhydrophobic silica aerogels, while no signals were observed in superhydrophilic silica aerogels (Fig. 4d). This confirmed that there are more ethyl groups on the hydrophobic aerogels than hydrophilic aerogels.

All results affirm the mechanism that esterification between Si-OH and ethanol induced the generation of hydrophobic Si-OCH₂CH₃ groups in 80 °C ethanol during fabrication of superhydrophobic silica aerogels. Hydrolysis of Si-OCH₂CH₃ into Si-OH in 80 °C water leads to the increasing ratio of hydrophilic groups during fabrication of superhydrophilic silica aerogels. Besides, it should be noted that esterification and hydrolysis are necessary but not sufficient conditions for achieving reversible SL-A/SB-A precursor transitions. M/T molar ratio and reaction time are two other important factors. When the M/T molar ratio is beyond 7:3 or below 4:6, there were no SL-A/SB-A precursor transitions within 72 h solvent treatment for silica gels. The superhydrophilicity or superhydrophobicity of the obtained aerogels are constant and can't be regulated by solvents (Supplementary Fig. 16). Because when MTMS is greatly excessive,

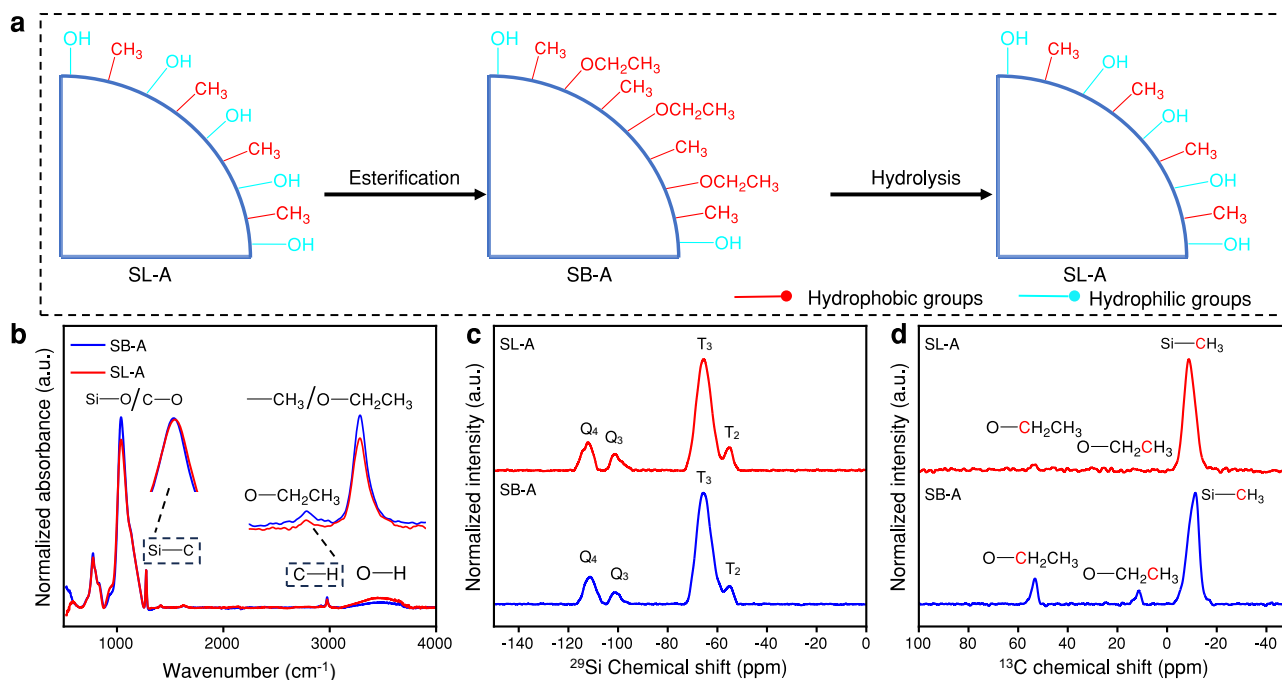


Fig. 4 | Mechanism investigation of switchable SL-A/SB-A precursor transitions. SB-A superhydrophobic aerogel, SL-A superhydrophilic aerogel. **a** Diagram illustration of solvent-regulable interfacial groups by reversible esterification reaction. **b** ATR-IR spectra, **c** ^{29}Si CP MAS NMR spectra, and **d** ^{13}C CP MAS NMR spectra of corresponding superhydrophobic/superhydrophilic silica aerogels (MTMS/TMOS

5:5) from SB-A/SL-A precursors. MTMS trimethoxymethylsilane, TMOS tetramethoxysilane. Qn denotes a tetrahedral Si with n bridging oxygens, Tn stands for a tetrahedral Si with 1C and n bridging oxygens. Source data are provided as a Source Data file.

the density of $-\text{CH}_3$ groups in the aerogel becomes excessive, resulting in a high proportion of hydrophobic groups and consequently yielding only hydrophobic aerogels either in ethanol or water. For example, water contact angle of silica aerogels synthesized with pure MTMS under ethanol as solvent can reach $152.7^\circ \pm 3.0^\circ$. After subjecting the silica SB-A precursor to water treatment at 80°C for 360 h, water contact angles of obtained silica aerogels still maintain $125.8^\circ \pm 2.6^\circ$ (Supplementary Fig. 17). Conversely, in the presence of a significant excess of TMOS, the density of $-\text{OH}$ in the aerogel becomes excessive, resulting in an inadequate generation of hydrophobic $-\text{OEt}$ within 72 h during esterification for the transition from hydrophilic aerogel precursors to hydrophobic aerogel precursors. (Fig. 1, Supplementary Fig. 18). For instance, the water contact angles of silica aerogels synthesized using pure TMOS as a precursor in ethanol solvent were found to be 0° . Even after subjecting the silica SB-A precursor to ethanol treatment at 80°C for 360 h, water contact angles of obtained silica aerogels remained unchanged at 0° (Supplementary Fig. 19). Besides the M/T molar ratio, the initial state of the precursor also affects the SL-A/SB-A precursor transition time. For example, compared with Fig. 2d, the SL-A precursor in Fig. 3c has a longer hydrophobic period. This may be due to that the SL-A precursor prepared with water as a solvent (Fig. 3c) has more surface $\text{Si}-\text{OH}$ groups than the SL-A precursor prepared by incomplete hydrolysis of the SB-A precursor (Fig. 2d).

Transitions universality and on-demand sorption

For the synthesis of silica aerogels, various silica precursors are commonly employed. The universality of solvent-regulated SB-A/SL-A precursor transitions and on-demand superhydrophobicity/superhydrophilicity of silica aerogels was validated by selecting different silica precursors, such as MTMS/TEOS and SMS/TMOS, with various molar ratios. (Fig. 5 a–c). For instance, the water contact angles of hydrophobic silica aerogels synthesized using molar ratios of MTMS/TEOS (7:3–4:6) ranged between $133.9^\circ \pm 2.0^\circ$ and $140^\circ \pm 1.4^\circ$.

Subsequent water treatment for SB-A precursor resulted silica aerogels with a reduction of the water contact angles to 0° , rendering the material completely hydrophilic (Fig. 5b). The silica aerogel prepared using SMS and TMOS exhibit a similar phenomenon. (Fig. 5c). These results indicate that not only precursors like MTMS and TMOS with such molar ratios, but also MTMS/TEOS and SMS/TMOS could fabricate silica aerogels with on-demand hydrophobicity/hydrophilicity (Supplementary Table 1).

Additionally, apart from ethanol, other alcohols such as methanol and isopropanol can also facilitate the formation of hydrophobic aerogels by converting SL-A precursors into SB-A precursors at 80°C for 72 h. However, only treatment with methanol and ethanol during the solvent treatment process induces the formation of hydrophobic aerogels exhibiting water contact angles of 152.8° and 151.8° respectively. On the contrary, isopropanol only results in aerogels with a water contact angle of 98.3° ; whereas isobutanol proves ineffective in achieving hydrophobization. (Supplementary Fig. 20) This phenomenon may be due to the different reactivity between alcohols and $\text{Si}-\text{OH}$ (methanol > ethanol > isopropanol > isobutanol)⁴³.

The application of aerogels in various scenarios is closely linked to the surface attribute of aerogels, encompassing adsorption⁴⁴, catalysis⁵, separation⁴⁵, filtration⁴⁶, surface modification³⁰, and more. Achieving on-demand superhydrophobicity/superhydrophilicity plays a pivotal role in enhancing the application adaptability of aerogels. For example, aerogels were usually used to adsorb dyes in water/oil mixtures⁴⁷. However, for unknown pigments and adsorption conditions, we need to evaluate and select aerogels with suitable surface attribute for efficient adsorption. In our model, we use methylene blue (MB) as dye, water as aqueous phase, and dichloromethane as the oil phase to evaluate the difference in dye adsorption capacity by silica aerogels with different surface attributes. Superhydrophobic silica aerogels exhibit superior adsorptive properties for MB in dichloromethane than superhydrophilic ones (Fig. 5d, e and Supplementary Fig. 21) as evidenced by the lower residual concentrations of MB in

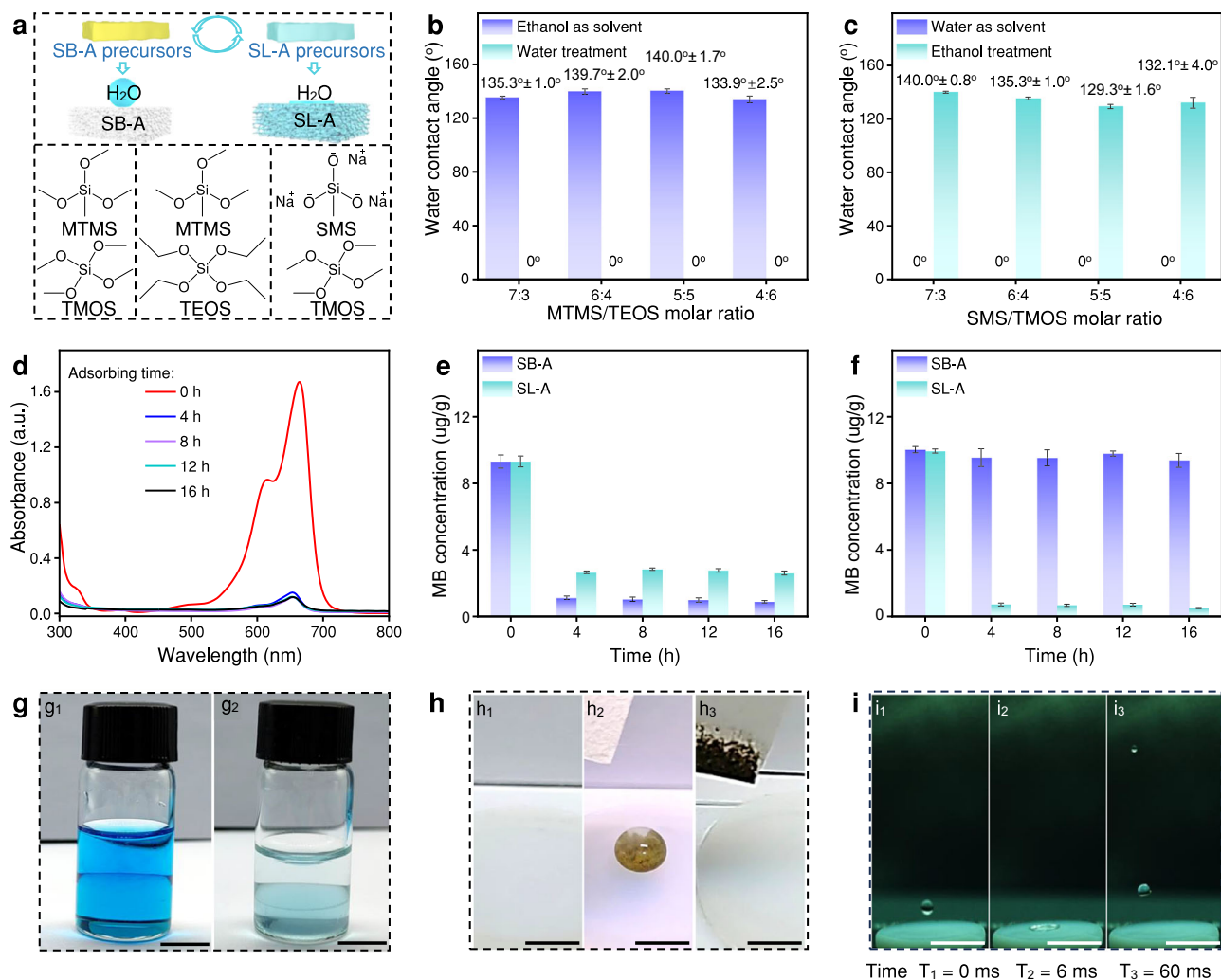


Fig. 5 | Universality of solvent-regulated SB-A/SL-A precursor transitions and on-demand application for corresponding superhydrophobic and superhydrophilic silica aerogels. SB-A superhydrophobic aerogel, SL-A superhydrophilic aerogel. **a** Chemical structures of diverse silica precursor mixtures for switchable SL-A/SB-A precursor transitions. MTMS trimethoxymethylsilane, TMOS tetramethoxysilane, TEOS tetraethyl orthosilicate, SMS sodium methicossilicate. **b** Water contact angles of MTMS/TEOS silica aerogels obtained from initial SB-A precursors and water-induced SL-A precursors. **c** Water contact angles of SMS/TMOS silica aerogels obtained from initial SL-A precursors and ethanol-induced SB-A precursors. **d** UV-vis spectra of residual MB in dichloromethane during adsorbing by superhydrophobic silica aerogels. MB: methylene blue. **e** Final residual

concentrations of MB in dichloromethane after adsorption by superhydrophobic silica aerogels and superhydrophilic ones. Error bar: <0.13 µg/g. **f** Final residual concentrations of MB in water after adsorption by superhydrophobic silica aerogels and superhydrophilic ones. Error bar: <0.53 µg/g. **g** Photographs of MB in dichloromethane (below layer) and water (upper layer) before adsorption (g_1) and after adsorption by superhydrophobic silica aerogels (below layer) and superhydrophilic ones (upper layer) (g_2). Scale bar: 1 cm. **h** Self-cleaning properties of superhydrophobic silica aerogels. Scale bar: 0.5 cm. **i** droplet resilience of superhydrophobic silica aerogels. Volume of water droplet is 10 µL. Scale bar: 1 cm. Source data are provided as a Source Data file.

dichloromethane after adsorption by the SB-As with residual concentration of 0.88 ppm compared to the superhydrophilic ones with residual concentration of 2.61 ppm, according to standard curves of dye concentration versus absorbance intensity (Supplementary Fig. 22). Nevertheless, only superhydrophilic silica aerogels can totally absorb MB in aqueous phase while superhydrophobic ones display negligible adsorption for dyes, with the residual concentrations of MB 0.50 ppm and 9.38 ppm respectively (Fig. 5f and Supplementary Fig. 23). The adsorption kinetics⁴⁸ of MB in oil and water suggest that the adsorption process is likely a synergy between physical adsorption and chemical adsorption (Supplementary Figs. 24–26 and Supplementary Table 2). The adsorption efficiency in oil-water mixing system can be enhanced by employing a combination of hydrophilic and hydrophobic aerogels, or by designing and applying aerogels with an appropriate level of surface attribute through controlled solvent treatment time. As exhibited in Fig. 5g, a clear solution was obtained

after MB in the oil phase being adsorbed by superhydrophobic silica aerogels and the dye in the aqueous phase being adsorbed by superhydrophilic ones (Fig. 5g₂).

Besides in dye adsorption, SB-As are generally considered to be suitable materials for self-cleaning, that can be disastrous for SL-As⁴⁹. As illustrated in Fig. 5h, muddy water on the surface of SB-As can be completely absorbed by absorbent paper without any residual pollutants. Moreover, once the falling water droplet touches the superhydrophobic surface of silica aerogels, it will rebound to a certain height (Fig. 5i and Supplementary Movie 1). While upon contact with muddy water, SL-As rapidly disintegrated, as depicted in Supplementary Fig. 27. All such results indicate self-cleaning property of superhydrophobic silica aerogels. Moreover, superhydrophobic silica aerogels also exhibit high oil-water separation efficiency in environments such as strong acids and bases (Supplementary Fig. 28 and Supplementary Table 3).

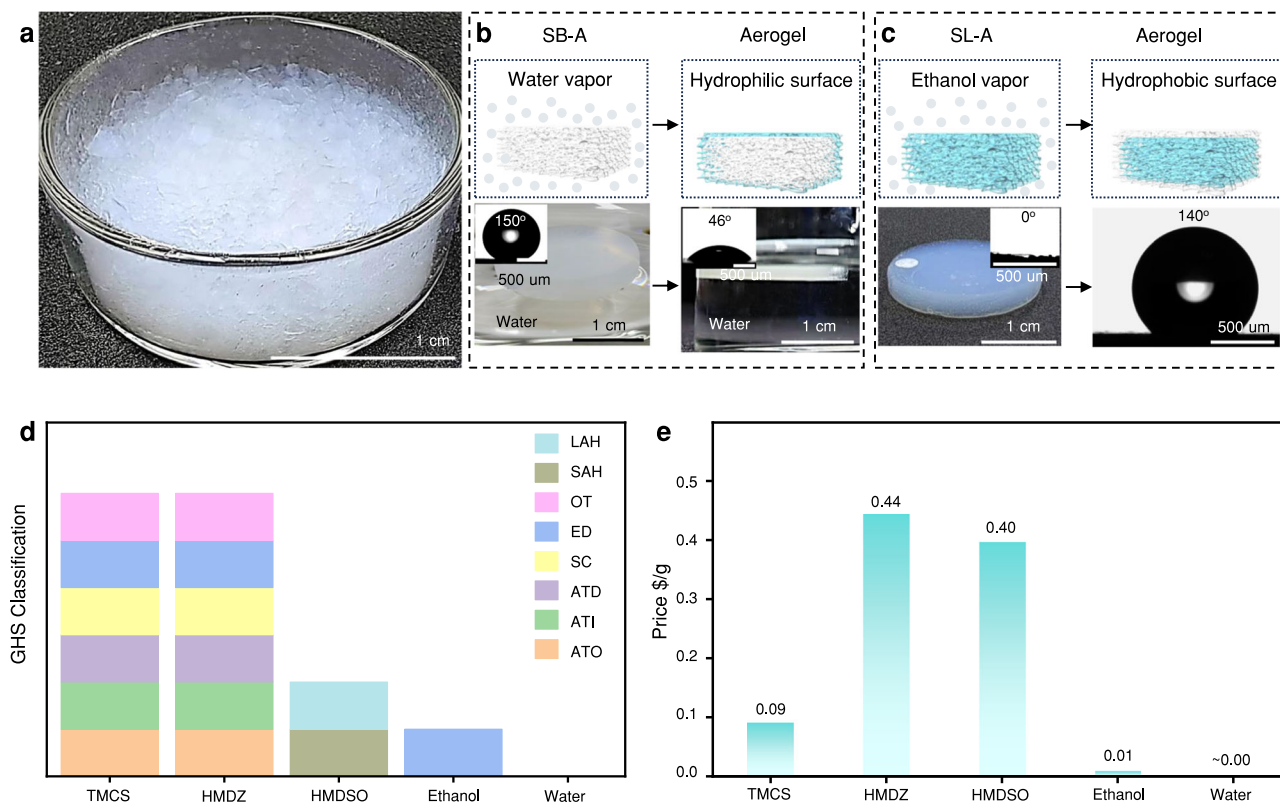


Fig. 6 | Comparison between traditional synthesis and our strategy. **a** Large-scale production of aerogels with our strategy. **b** Hydrophobic aerogel to hydrophilic one in water vapor. SB-A superhydrophobic aerogel. **c** Hydrophilic aerogel to hydrophobic one in ethanol vapor. SL-A superhydrophilic aerogel. **d** Physiological toxicity of common hydrophobic modification reagents used elsewhere and solvents used in this work. GHS classification Globally Harmonized System of Classification and Labeling of Chemicals, SAH/LAH short/long-term (acute/chronic)

aquatic hazard, OT specific target organ toxicity, ED serious eye damage/irritation, SC skin corrosion/irritation, ATD acute toxicity (dermal), ATI acute toxicity (inhalation), ATO acute toxicity (oral), TMCS trimethylchlorosilane, HMDZ hexamethylsilazane, HMDSO hexamethyldisiloxane. **e** Cost of common hydrophobic modification reagents used elsewhere and solvents used in this work. Source data are provided as a Source Data file.

Comparison between traditional synthesis and our strategy

Compared to the conventional hydrophobic modification method of silica aerogels, the utilization of water/ethanol for solvent-regulated surface attributes in aerogels offers significant advantages. Currently, the conventional hydrophobic modification of silica aerogels typically involves the addition of hydrophobic modification reagents to the reaction system⁵⁰, thereby necessitating a subsequent complex process to remove excess reagents. In contrast, this study demonstrates a more convenient and simplified approach by achieving switchable hydrophilic and hydrophobic modification through direct solvent heating. Based on this, we can realize the rapid and large-scale modification of hydrophilic and hydrophobic aerogels (Fig. 6a).

Moreover, the conventional hydrophobic reaction of silica aerogels involves the utilization of a reactant containing hydrophobic groups to interact with the functional groups of silica⁵¹. This reaction is typically irreversible, thereby enabling solely hydrophobic modification while precluding any possibility of achieving hydrophilic modification. In this study, in addition to the switchable hydrophilic and hydrophobic modification in the liquid phase mentioned above, we also demonstrate the feasibility of achieving hydrophilic and hydrophobic modification in the gas phase. Under normal service environment, superhydrophobic silica aerogels show excellent hydrophobic stability (even at 100% humidity and 60–80 °C. Supplementary Fig. 29) and mechanical property stability. For example, the mechanical properties of silica samples remain unchanged after multiple precursor cycles, superhydrophilic-superhydrophobic conversion, and prolonged outdoor use

(Supplementary Figs. 30–33 and Supplementary Tables 4–6). After 125 °C hot water steam treatment, the SB-A with the original capability of floating on the aqueous interface was immersed into water, indicating a transition from hydrophobicity to hydrophilicity on the aerogel surface with water contact angle changed from 148.0° to 46° (Fig. 6b). After subjecting the hydrophilic aerogel to high-temperature ethanol treatment, a notable transition from hydrophilicity with water contact angle 0° to hydrophobicity was observed, as evidenced by water contact angle 140° (Fig. 6c). This means that switchable hydrophobic modification of silica aerogel surfaces can be rapidly and efficiently achieved through this approach, eliminating the need for time-consuming solvent displacement and drying processes. Additionally, according to the Safety Data Sheet (Supplementary Table 7), the most hydrophobic modification agents are expensive and exhibit physiological toxicity such as acute toxicity, (oral/inhalation/dermal) (ATO/ATI/ATD), skin corrosion/irritation (SC), serious eye damage/irritation (ED), specific target organ toxicity (OT), short/long-term (acute/chronic) aquatic hazard (SAH/LAH). In contrast, compared to trimethylchlorosilane (TMCS), hexamethyldisilazane (HMDZ), hexamethyldisiloxane (HMDSO), etc. as the modification reagents⁵², ethanol and water are considered cost-effective and green solvents (Fig. 6d, e). Moreover, SB-As with static water contact angle (150.7°) and water sliding angle (3.3°) can also be obtained through ambient drying, showing specific surface area of 1084 m²/g without the need for Sc CO₂ drying (Supplementary Fig. 34). This indicates that this work is at the same time a more green and economical hydrophobic modification method of silica aerogels. In summary, this work offers

an environmentally friendly, cost-effective, and efficient approach for achieving switchable hydrophilic-hydrophobic modification.

Discussion

In summary, silica aerogels with on-demand superhydrophobic/superhydrophilic properties are synthesized by precisely controlling the solvent composition (water/ethanol) during sol-gel transition and solvent exchange process. Reversible transitions between SB-A precursor and SL-A precursor induced by solvent exchange in ethanol and water respectively at 80 °C leads to on-demand superhydrophobic/superhydrophilic properties of silica aerogels. Changes either in synthetic routes or silica precursors, solvent-regulated SB-A/SL-A precursor transitions, and on-demand superhydrophobicity and superhydrophilicity consistently occur during the preparation of silica aerogels, demonstrating their universality. Mechanistic studies reveal that these switchable transitions are attributed to reversible esterification reactions between Si-OH groups and ethanol. Such solvent-regulable interfacial groups enable on-demand superhydrophobic/superhydrophilic silica aerogels in various applications including adsorption, etc. In conclusion, this article unveils a long-overlooked phenomenon: solvent-induced hydrophobization and hydrophilization in the field of silica aerogels, which serves as a significant wake-up call for practitioners working with these materials. Furthermore, this discovery offers an environmentally friendly, cost-effective, and efficient approach for aerogels to achieve switchable hydrophilic-hydrophobic modifications.

Methods

Materials

Trimethoxymethylsilane (MTMS) (98%), Tetramethoxysilane (TMOS) (98%), and Tetraethyl orthosilicate (TEOS) (98%), Hydrochloric acid (HCl) (37%), Ammonia aqueous solution ($\text{NH}_3\cdot\text{H}_2\text{O}$, 28–30%, ACS), Ethanol (ACS $\geq 99.5\%$), Methylene blue (Indicator grade) and Dichloromethane (AR, 99.5%) are purchased from Aladdin Industrial Corporation (Shanghai, China). Acetone ($\geq 99.0\%$) is purchased from Sinopharm Chemical Reagent Co., Ltd (Shanghai, China).

Sodium methicosilicate (SMS) (AR, 30%) is purchased from Yuan-ye Bio-Technology Co., Ltd (Shanghai, China). Deionized water ($18.2 \text{ M}\Omega \text{ cm}^{-1}$) was obtained from a Millipore-Q system. All other reagents were used without further purification.

Synthesis of the silica aerogels by MTMS and TMOS. To prepare silica aerogels, 2 mmol silica precursors with diverse molar ratios of MTMS and TMOS are added into 1 mL ethanol or water and followed with 130 μL 0.01 mol/L HCl and then stirred for 30 min at room temperature to form silica sol. Then 87 μL 2 mol/L $\text{NH}_3\cdot\text{H}_2\text{O}$ are added into the above sol and put at 80 °C for 2 days for sol-gel transitions and then complete gelling and aging processes to form silica organogel and hydrogel. Residues are removed before solvent treatment process. Solvent treatment process are based on replacing ethanol in organogel with 20 mL water 3 times to form hydrogel at 80 °C for diverse time periods or exchange water in hydrogel with 20 mL ethanol for 3 times to form organogel at 80 °C for diverse time periods.

Synthesis of the silica aerogels by MTMS and TEOS. To hydrolyze TEOS, 1 mol TEOS and 34.2 mL 0.01 mol/L HCl were added to 234 mL ethanol and then stirred at 130 °C for 8 h to get transparent TEOS solution. To get silica organogel, 2 mmol silica precursors with diverse molar ratios of MTMS and TEOS are added into 1 mL ethanol and followed with 130 μL 0.01 mol/L HCl and stirred for 30 min at room temperature. Eighty-seven microlitre 2 mol/L $\text{NH}_3\cdot\text{H}_2\text{O}$ are added and put at 80 °C for 2 days to form organogel. Residues are removed before solvent treatment process.

Solvent treatment process is based on replacing ethanol in organogel with 20 mL water for 3 times to form hydrogel at 80 °C for 72 h.

Synthesis of the silica aerogels by SMS and TMOS. To get silica hydrogel, 2 mmol silica precursors with diverse molar ratios of SMS and TMOS are added into 1 mL water and followed with 360 μL 10 mol/L HCl and put at 80 °C for 2 days for sol-gel transitions to form hydrogel. Sodium salt was removed by water before solvent treatment process. Solvent treatment process is based on replacing water in hydrogel with 20 mL ethanol for 3 times to form organogel at 80 °C for 72 h.

Synthesis of the silica aerogels by MTMS. To prepare pure MTMS silica aerogels, 2 mmol MTMS are added into 1 mL ethanol and followed with 130 μL 0.01 mol/L HCl and then stirred for 30 min at room temperature to form silica sol. Then 87 μL 2 mol/L $\text{NH}_3\cdot\text{H}_2\text{O}$ are added into the above sol and put at 80 °C for 2 days for sol-gel transitions and then complete gelling and aging processes to form silica organogel. Residues are removed before solvent treatment process. Solvent treatment process is based on replacing ethanol in silica organogel with 20 mL water for 3 times to form hydrogel at 80 °C for diverse days.

Synthesis of the silica aerogels by TMOS

To prepare pure TMOS silica aerogels, 2 mmol TMOS are added into 1 mL ethanol and followed with 130 μL 0.01 mol/L HCl and then stirred for 30 min at room temperature to form silica sol. Then 87 μL 2 mol/L $\text{NH}_3\cdot\text{H}_2\text{O}$ are added into the above sol and put at 80 °C for 2 days for sol-gel transitions and then complete gelling and aging processes to form TMOS silica organogel. Residues are removed before solvent treatment process. Solvent treatment process is based on replacing ethanol in TMOS silica organogel with 20 mL ethanol for 3 times to form TMOS silica organogel at 80 °C for diverse days.

Detailed Sc drying conditions. Sc CO_2 drying is generally applied to get silica aerogel in industry. In order to get ideal silica aerogel structure, ethanol is commonly selected as an exchange solvent for gels before putting them in Sc reactor. In order to exclude the influence of ethanol on aerogel properties during Sc drying, all wet gels were solvent exchanged with acetone before Sc drying at least 6 times at room temperature for 2 days to ascertain complete removal of ethanol before Sc drying (Supplementary Fig. 35). Acetone gel was dried in circulating Sc CO_2 fluids at 40 °C and 10 MPa for at least 10 h with a flow rate exceeding 6 L/h to ensure complete replacement of acetone by Sc CO_2 fluid. Depressurization was initiated only after no further release of acetone from the gas vent and continued for at least 5 h to facilitate degassing. Under these optimized conditions, our aerogels exhibited no residual traces of acetone.

Dye adsorption. Prepare 0.010 mg/g methylene blue aqueous solution and 0.010 mg/g methylene blue/dichloromethane solution, respectively. Thirty milligrams SL or SB-A were used to adsorb dye in a 3 g solution for various periods. Then detect residue concentration of methylene blue in solution by UV-vis. Three samples were tested to calculate the average value and standard deviations. Calculation of dye concentration is based on establishing a standard curve between absorbance intensity and dye of known concentration based on the Lambert-Beer law, which means a linear correlation between the absorbance intensity and dye concentration.

Separation efficiency of oil-water emulsion. The oil in water emulsion was prepared by adding 5 mL n-hexane, 0.1 g Tween 80 into 95 mL water and stirred for 2 h. Add 80 mg superhydrophobic silica aerogel into 5 mL oil in water emulsion prepared before and stir for 2 h to remove oil in emulsion. The pH value of 5 mL oil in water emulsion is regulated by adding 20 μL HCl to reach pH = 2 or ammonia to reach pH = 13. Then analyze the total organic carbon (TOC) content of the emulsion before and after separation by the TOC Analyzer. All samples were diluted by 200 times by adding 200 μL sample solution into

20 mL water (v/v). Three samples were tested to calculate the average value and standard deviation.

Oil-water separation can be calculated by testing TOC concentration before and after emulsion separation. The equation of separation efficiency⁵³ can be determined as:

$$R = [(C_0 - C) / C_0] \times 100\% \quad (1)$$

Here, R represents the separation efficiency, C_0 and C means the TOC concentration in the emulsion before separation and after separation.

Characterization. Water contact angles of silica aerogels are tested by an optical contact angle goniometer (OCA 15EC, Data Physics Instruments, Germany) with 5 μ L water. The static water contact angle and water sliding angle of droplets on sample surface were started to be measured after the water droplet contacted the surface of the samples for 20 s. Water sliding angle were tested by tilting the surfaces at a slow rate of 0.1°/s and the water sliding angle is defined as critical tilted angle which droplets start the continuous motion on the sample surface within 1 s. Three samples were tested to calculate the average value and standard deviation. Specific surface areas and pore size distributions are tested by the BET and Barrett–Joyner–Halenda methods based on nitrogen adsorption and desorption curves (ASAP 2020, Micromeritics, USA). Aerogels need to be outgassed at 120 °C for 4 h before further measurements. Three samples were tested to calculate the average value and standard deviation. The micro-morphologies and microstructures of silica aerogels are characterized by scanning electron microscopy (SEM, Hitachi S-4800, Japan) at 5 kV acceleration voltage. Size distribution of secondary particles of silica aerogel was analyzed by Nano Measure software based on the captured SEM images²⁹. Si and ¹³C superconducting NMR spectra are tested by a solid superconducting NMR spectrometer (NMR, JEOL JNM-ECZ600R, Japan) at 80.0 Hz. Chemical structure of silica aerogels are measured by a Fourier Transform Infrared Spectroscopy (FTIR, 5700, FL, USA) equipped with attenuated total reflection (ATR) accessory over 64 scans measured with a resolution wavelength of 4 cm⁻¹. Both superhydrophobic and SL-A samples were dried in a vacuum oven prior to testing and subsequently tested and analyzed in a dry environment quickly. During data analysis, the interference peak from water vapor in the background air was corrected. Consequently, the likelihood of hydroxyl vibration deviation due to atmospheric moisture during testing is minimal. Dynamic process of water droplets is captured by high-speed camera (VW-9000C) with 5 μ L water dropping from a height of 20 cm. Absorbance of methylene blue solution is measured by an Ultraviolet-visible near infrared spectroscopy (UV–vis–NIR, Cary5000, Agilent, USA) within range of 300–900 nm. Gas chromatogram of acetone and ethanol mixture is measured by the gas chromatograph-mass spectrometer (GC-MS QP2010SE, SIMADZU) with Rtx-5MS chromatographic column and gas temperature holds at 40 °C for 1 min and then increase at 5 °C/min to 200 °C and then maintain for 5 min to test samples. Morphologies and size distribution of primary particles of silica aerogel were characterized on a Tecnai G2 F20 S-TWIN high-resolution transmission electron microscopy (FEI, USA) (TEM) with 200 kV acceleration voltage. Size distribution of primary particles of silica aerogel was analyzed by Nano Measure software based on the captured TEM images. The sample was prepared by homogeneously dispersing the silica aerogel in ethanol and ultrasonically for 2 h. Then dipping the dispersion onto the thin carbon film and drying it in a vacuum oven for 6 h. The mechanical properties of aerogels were tested by a tensile testing machine (Instron 3365, ITW, USA). The measured sample for a compression test is a cylinder with a height of 7 mm and a radius of 23 mm. Three samples were tested to calculate the average value and standard deviation. The surface roughness of the samples was measured by 3D confocal microscopy

with magnification ($\times 150$) (VK-X200, Keyence) by focusing on the surface of the samples. The captured images are 95 μ m on x -axis and 75 μ m on y -axis. Three samples were tested to calculate the average value and standard deviation. TOC content of oil in water emulsion before and after separation by silica aerogel was analyzed by the TOC Analyzer (O-I-Analytical, USA).

Data availability

The data supporting the findings are provided within this Article and its Supplementary Information. Extra data are available from the corresponding authors upon request. Source data are provided with this paper.

References

- Sheng, Z. et al. The rising aerogel fibers: status, challenges, and opportunities. *Adv. Sci.* **10**, 2205762 (2023).
- Wu, M. et al. Biomimetic, knittable aerogel fiber for thermal insulation textile. *Science* **382**, 1379–1383 (2023).
- Guo, J. et al. Hypocrystalline ceramic aerogels for thermal insulation at extreme conditions. *Nature* **606**, 909–916 (2022).
- Li, D. et al. Double-helix structure in carrageenan–metal hydrogels: a general approach to porous metal sulfides/carbon aerogels with excellent sodium-ion storage. *Angew. Chem. Int. Ed.* **55**, 15925–15928 (2016).
- Li, Z. et al. Atomic aerogel materials (or single-atom aerogels): an interesting new paradigm in materials science and catalysis science. *Adv. Mater.* **35**, 2211221 (2023).
- Ali, E. et al. Giant-stroke, superelastic carbon nanotube aerogel muscles. *Science* **5921**, 1575–1578 (2009).
- Wang, C. et al. Closed-loop recyclable high-performance polyimine aerogels derived from bio-based resources. *Adv. Mater.* **35**, 2209003 (2023).
- Li, C. et al. Silica aerogels: from materials research to industrial applications. *Int. Mater. Rev.* **68**, 862–900 (2023).
- Wang, F. et al. Biomimetic and superelastic silica nanofibrous aerogels with rechargeable bactericidal function for antifouling water disinfection. *ACS Nano* **14**, 8975–8984 (2020).
- Zhao, S. et al. Additive manufacturing of silica aerogels. *Nature* **584**, 387–392 (2020).
- Ji, X. et al. Ratio-tuning of silica aerogel co-hydrolyzed precursors enables broadband, angle-independent, deformation-tolerant, achieving 99.7% reflectivity. *Small* **19**, 2301534 (2023).
- Mazrouei-Sebdani, Z. et al. A review on silica aerogel-based materials for acoustic applications. *J. Non Cryst. Solids* **562**, 120770 (2021).
- Lin, J. et al. A review of recent progress on the silica aerogel monoliths: synthesis, reinforcement, and applications. *J. Mater. Sci.* **56**, 10812–10833 (2021).
- Welsch, T. et al. Comparison of different aerogel granules for use as aggregate in concrete. *Gels* **9**, 406 (2023).
- Pan, Y. et al. A fast synthesis of silica aerogel powders-based on water glass via ambient drying. *J. Sol Gel Sci. Technol.* **82**, 594–601 (2017).
- Nocentini, K. et al. Hygro-thermal properties of silica aerogel blankets dried using microwave heating for building thermal insulation. *Energy Build.* **158**, 14–22 (2018).
- Tian, Y. et al. Ionic liquid-functionalized silica aerogel as coating for solid-phase microextraction. *J. Chromatogr. A* **1583**, 48–54 (2019).
- Jones, S. M. Aerogel: space exploration applications. *J. Sol Gel Sci. Technol.* **40**, 351–317 (2006).
- Iijima, T. et al. Aerogel Cherenkov counter for the BELLE detector. *Nucl. Instrum. Methods Phys. Res. A* **453**, 321–325 (2000).
- Li, L. et al. Thermal-responsive, super-strong, ultrathin firewalls for quenching thermal runaway in high-energy battery modules. *Energy Storage Mater.* **40**, 329–336 (2021).

21. Erdem, C. et al. Toward aerogel based thermal superinsulation in buildings: a comprehensive review. *Renew. Sust. Energy Rev.* **34**, 273–299 (2014).
22. Mendes, A. L. et al. Progress in silica aerogel-containing materials for buildings' thermal insulation. *Constr. Build. Mater.* **286**, 122815 (2021).
23. Lukas, H. et al. Fast and minimal-solvent production of super-insulating silica aerogel granulate. *Angew. Chem. Int. Ed.* **56**, 4753–4756 (2017).
24. Zhao, L. et al. Harnessing heat beyond 200 °C from unconcentrated sunlight with nonevacuated transparent aerogels. *ACS Nano* **13**, 7508–7516 (2019).
25. Ji, X. et al. Elaborate size-tuning of silica aerogel building blocks enables laser-driven lighting. *Adv. Mater.* **34**, 2107168 (2022).
26. Wang, L. et al. Structural characteristics and thermal conductivity of ambient pressure dried silica aerogels with one-step solvent exchange/surface modification. *Mater. Chem. Phys.* **113**, 485–490 (2009).
27. Jansson, H. et al. Silicate species of water glass and insights for alkali-activated green cement. *AIP Adv.* **5**, 67167 (2015).
28. Estella, J. et al. Effect of supercritical drying conditions in ethanol on the structural and textural properties of silica aerogels. *J. Porous Mater.* **15**, 705–713 (2008).
29. Gurikov, P. et al. 110th anniversary: solvent exchange in the processing of biopolymer aerogels: current status and open questions. *Ind. Eng. Chem. Res.* **58**, 18590–18600 (2019).
30. Schubert, U. et al. Aerogels—airy materials: chemistry, structure, and properties. *Angew. Chem. Int. Ed.* **37**, 22–45 (1998).
31. Schubert, U. et al. Influence of supercritical drying fluid on structure and properties of organically modified silica aerogels. *J. Non Cryst. Solids.* **186**, 37–43 (1995).
32. Du, Y. et al. Reaction-spun transparent silica aerogel fibers. *ACS Nano* **14**, 11919–11928 (2020).
33. Rahul, D. M. et al. Creation of “Rose Petal” and “Lotus Leaf” effects on alumina by surface functionalization and metal-ion coordination. *Angew. Chem. Int. Ed.* **56**, 16018–16022 (2017).
34. Almonte, L. et al. Rose petal effect: a subtle combination of nano-scale roughness and chemical variability. *Nano Select* **3**, 977–989 (2022).
35. Zhang, J. et al. Durable superhydrophobic surfaces with self-generated wenzel sites for efficient fog collection. *Small* **20**, 2312112 (2024).
36. Rao, A. P. et al. Modifying the surface energy and hydrophobicity of the low-density silica aerogels through the use of combinations of surface-modification agents. *J. Mater. Sci.* **45**, 51–63 (2010).
37. Socrates, G. *Infrared and Raman Characteristic Group Frequencies: Tables and Charts* 3rd edn (Wiley, 2001).
38. Günzler, H. et al. *IR spectroscopy: An Introduction* 178–183 (Wiley-VCH, 2002).
39. Al-Oweini, R. et al. Synthesis and characterization by FTIR spectroscopy of silica aerogels prepared using several Si(OR)₄ and R⁺Si(OR)₃ precursors. *J. Mol. Struct.* **919**, 140–145 (2009).
40. Jyoti, L. et al. Ambient pressure dried TEOS-based silica aerogels: good absorbers of organic liquids. *J. Mater. Sci.* **45**, 503–510 (2010).
41. Malfait, W. J. et al. Surface chemistry of hydrophobic silica aerogels. *Chem. Mater.* **27**, 6737–6745 (2015).
42. Wim, J. M. et al. Hydrophobization of silica aerogels: insights from quantitative solid-state NMR spectroscopy. *J. Phys. Chem. C* **118**, 25545–25554 (2014).
43. Kimura, T. et al. Esterification of the silanol groups in the mesoporous silica derived from kanemite. *J. Porous Mater.* **5**, 127–132 (1998).
44. Cao, C. et al. Robust fluorine-free superhydrophobic PDMS–ormosil@fabrics for highly effective self-cleaning and efficient oil–water separation. *J. Mater. Chem. A* **4**, 12179–12187 (2016).
45. Pan, Y. et al. Surfaces with controllable super-wettability and applications for smart oil water separation. *Chem. Eng. J.* **378**, 122178 (2019).
46. Amonette, J. E. et al. Functionalized silica aerogels for gas-phase purification, sensing, and catalysis: a review. *Microporous Mesoporous Mater.* **250**, 100–119 (2017).
47. Abolghasemi Mahani, A. et al. Sol-gel derived flexible silica aerogel as selective adsorbent for water decontamination from crude oil. *Mar. Pollut. Bull.* **129**, 438–447 (2018).
48. Jiang, H. et al. Liquid-in-aerogel porous composite allows efficient CO₂ capture and CO₂/N₂ separation [J]. *Small* **19**, 2302627 (2023).
49. Ren, J. et al. Transparent, robust, and machinable hybrid silica aerogel with a “rigid-flexible” combined structure for thermal insulation, oil/water separation, and self-cleaning. *J. Colloid Interface Sci.* **623**, 1101–1110 (2022).
50. Mahadik, D. B. et al. Effect of concentration of trimethylchlorosilane (TMCS) and hexamethyldisilazane (HMDZ) silylating agents on surface free energy of silica aerogels. *J. Colloid Interface Sci.* **356**, 298–302 (2011).
51. Nihei, T. et al. Dental applications for silane coupling agents. *J. Oral Sci.* **58**, 151–155 (2016).
52. Gurav, J. L. et al. Effect of mixed catalysts system on TEOS-based silica aerogels dried at ambient pressure. *Appl. Surf. Sci.* **255**, 3019–3027 (2008).
53. Zhang, J. et al. Membrane wettability manipulation via mixed dimensional heterostructured surface towards highly efficient oil-in-water emulsion separation [J]. *J. Membr. Sci.* **672**, 121472 (2023).

Acknowledgments

We are grateful for the support from the National Natural Science Foundation of China (Project 52173052 to X.Z.; 52203021 to L.L.) and the Natural Science Foundation of Jiangsu Province (Project BK20220296 to L.L.).

Author contributions

X.Z., L.C., and L.L. conceived the idea and designed the experiments. X.Z. supervised the project. L.C. conducted the experiments and the data were analysed and processed by X.Z., L.L., and L.C. L.C. prepared the manuscript, and X.Z. and L.L. revised the manuscript.

Competing interests

The authors declare no competing interests.

Additional information

Supplementary information The online version contains supplementary material available at <https://doi.org/10.1038/s41467-025-57246-2>.

Correspondence and requests for materials should be addressed to Xueting Zhang.

Peer review information *Nature Communications* thanks Chaobo Huang, Xudong Jia, and the other, anonymous, reviewer(s) for their contribution to the peer review of this work. A peer review file is available.

Reprints and permissions information is available at <http://www.nature.com/reprints>

Publisher's note Springer Nature remains neutral with regard to jurisdictional claims in published maps and institutional affiliations.

Open Access This article is licensed under a Creative Commons Attribution-NonCommercial-NoDerivatives 4.0 International License, which permits any non-commercial use, sharing, distribution and reproduction in any medium or format, as long as you give appropriate credit to the original author(s) and the source, provide a link to the Creative Commons licence, and indicate if you modified the licensed material. You do not have permission under this licence to share adapted material derived from this article or parts of it. The images or other third party material in this article are included in the article's Creative Commons licence, unless indicated otherwise in a credit line to the material. If material is not included in the article's Creative Commons licence and your intended use is not permitted by statutory regulation or exceeds the permitted use, you will need to obtain permission directly from the copyright holder. To view a copy of this licence, visit <http://creativecommons.org/licenses/by-nc-nd/4.0/>.

© The Author(s) 2025